

Keywords

Thermoluminescence,
Otor Model,
Numerical Solution,
Runge-Kutta

Received: October 30, 2017

Accepted: November 16, 2017

Published: December 6, 2017

On the Numerical Solution of the One Trap One Recombination Model for First Order Kinetic

Erdem Uzun

Department of Physics, Karamanoğlu Mehmetbey University, Karaman, Turkey

Email address

erdemuzun@kmu.edu.tr

Citation

Erdem Uzun. On the Numerical Solution of the One Trap One Recombination Model for First Order Kinetic. *AASCIT Journal of Physics*. Vol. 3, No. 5, 2017, pp. 36-43.

Abstract

One trap one recombination center model was proposed to explain thermoluminescence emission and it should be emphasized that the model has its own allowed charge carrier transitions, trapping parameters and differential equations set. The equations are not linear and thus analytical solutions are not possible. Therefore, numerical solutions of the thermoluminescence equations have been effectively used in thermoluminescence studies. In this paper the one trap one recombination center model is solved, numerically by using Explicit Euler, Generalized Euler, Classical Runge-Kutta, Implicit Runge-Kutta and Explicit Runge-Kutta methods for different step sizes and differential orders. In order to comparison of the simulations, some experiments are also performed. Moreover, experimental trap parameters are used as initial conditions in the simulations. Because working precision is held as many digits throughout the numerical solutions, very precise figure of merit values are calculated. Number of simulations show that when difference between the FOM values, which calculated by using various numerical methods, are very small, the shortness of calculation time seems to be a good criterion in the choice of method.

1. Introduction

Thermoluminescence (TL) event is well established with several physical models. Moreover, charge carrier concentrations and TL intensities are given by differential equation sets. Although the models are relatively basic, analytic solutions of the differential equations are not possible. Therefore, approximate numerical simulations must be performed for the comparisons of the experimental measurements and models. Numerical solutions of the TL equations are widely used in TL applications. Pros and cons arguments of the numerical solutions of the TL equations were argued by McKeever [1] and Chen and McKeever [2] and Chen and Pagonis [3]. The first numerical approximation of the TL equations was performed by Kemmey et al [4] and numerical solutions were given by Kelly et al [5] for the first time. Moreover, Shenker and Chen [6], Chen et al [7] and many others have published numerical solutions of the TL equations up to now.

Lots of numerical methods are available such as Euler Methods and Runge Kutta Methods for numerical solutions of differential equations. Each numerical methods uses own adaptive procedures such as size of the steps and sums of products of partial derivatives. Commonly, numerical solutions of the differential equations start at a particular values of variables (such as appropriate initial conditions) and then takes a sequence of steps to find solutions iteratively. Nevertheless, some of the methods give faster results and the others give more precise results. An intelligent approach is to

choose sufficiently precise and fast method. Besides, success of the numerical calculation is controlled by FOM values [8] between calculated and experimental glow curves [9]. Therefore, it is desirable that the FOM value is at the lowest possible value for a good fit.

In this paper, one trap one recombination (OTOR) model are chosen and numerical solutions of its differential equations set are performed. For this purpose, we apply Explicit Euler, Generalized Euler, Classical Runge-Kutta (3-9 order), Implicit Runge-Kutta (3-9 order), Explicit Runge-Kutta (3-8 order), Explicit Runge-Kutta with Fehlberg Coefficients (3-9 order), Explicit Runge-Kutta with Bogacki-Shampine Coefficients (3-9 order) methods to OTOR model. All numerical simulations are performed in Mathematica 8.1. Besides, an experimental first ordered glow curve is measured and its TL trap parameters are determined. Results are compared with numerical glow curve and figure of merit (FOM) are calculated.

2. Method

2.1. OTOR Model

According to the OTOR model (Figure 1) there are three allowed transitions are available; trapped electrons can be

$$\frac{dn_c}{dt} = n_s s_e \exp\left\{-\frac{E_e}{k.T}\right\} - n_c (N - n) A_{te} - n_c (n + n_c) A_{re} \quad (1)$$

$$\frac{dn}{dt} = n_c (N - n) A_{te} - n s_e \exp\left\{-\frac{E_e}{k.T}\right\} \quad (2)$$

$$I_{TL} = -\eta n_c (n + n_c) A_{re} \quad (3)$$

Here, A_{te} and A_{re} are re-trapping and recombination probability coefficients and η is the radiative efficiency. If all recombination causes photon emission and all photons are detected, η is approximately equal to 1. If $A_{re}=1$ and $A_{te}=0$ is taken, otor model can be represent experimental first order glow curve.

2.2. Experimental Methods

Samples used in this study is α -Al₂O₃ powder. α -Al₂O₃ has four TL peaks and the first peak is located at 117±2°C. In order to isolate of the first peak, some experimental procedures are performed. Firstly, α -Al₂O₃ sample is annealed at 600°C for 15 min to erase any residual radiation effects. Then, it is spread on thin aluminum disk about 10mg and it is irradiated at room temperature using the beta rays from a calibrated ⁹⁰Sr-⁹⁰Y source. Full glow curve of the sample is recorded between 40-400°C temperature ranges

released by thermally; free electrons are trapped by N or recombined. Here, N is trapping states (in cm⁻³) and with instantaneous occupancy n. The activation energy for the electron trap is E_e (in eV) and the frequency factor is s_e (s⁻¹). k is the Boltzmann constant (k = 8.617×10⁻⁵ eV K⁻¹)

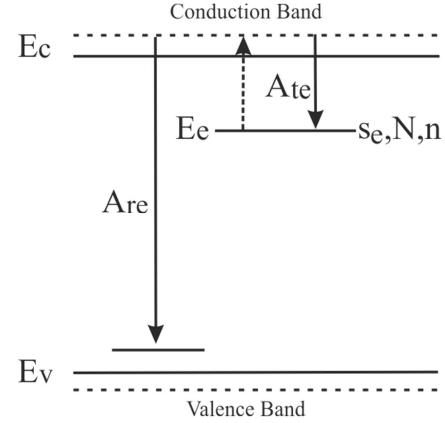


Figure 1. Schematic energy level diagram of otor model.

Differential equations representing the charge carrier traffic as a function of temperature and time are given:

using linear heating rate as reference. Thereafter, the annealing and irradiation procedure repeated. The sample is heated up to T_s and cooled to room temperature. Lastly, full glow curve of the sample is recorded again. Last glow curve is subtracted from the reference and the peak is obtained in isolated manner. The procedures are repeated several times for different T_s. T_s's are chosen between 100°C-140°C. After then trap parameters are calculated by using peak shape, various heating rate (β=1-3°C/s) and initial rise methods. The details of the methods can be found in books and reviews. n₀ value is calculated as area under the experimental glow curve in Figure 3. Results are given in Table 1. The experimental trap parameters given in Table 1 are the average values of the experimental results of all the calculation methods. TL glow curve of the α -Al₂O₃ is show in Figure 2 and isolated first peak is shown in Figure 3.

Table 1. Experimental trap parameters.

	E _e (eV)	S _e (s ⁻¹)	n ₀ (cm ⁻³)	I _{max} (counts)	b
FOK peak	0.89±0.02	2.17±0.07×10 ¹⁰	117286	3130	1.00

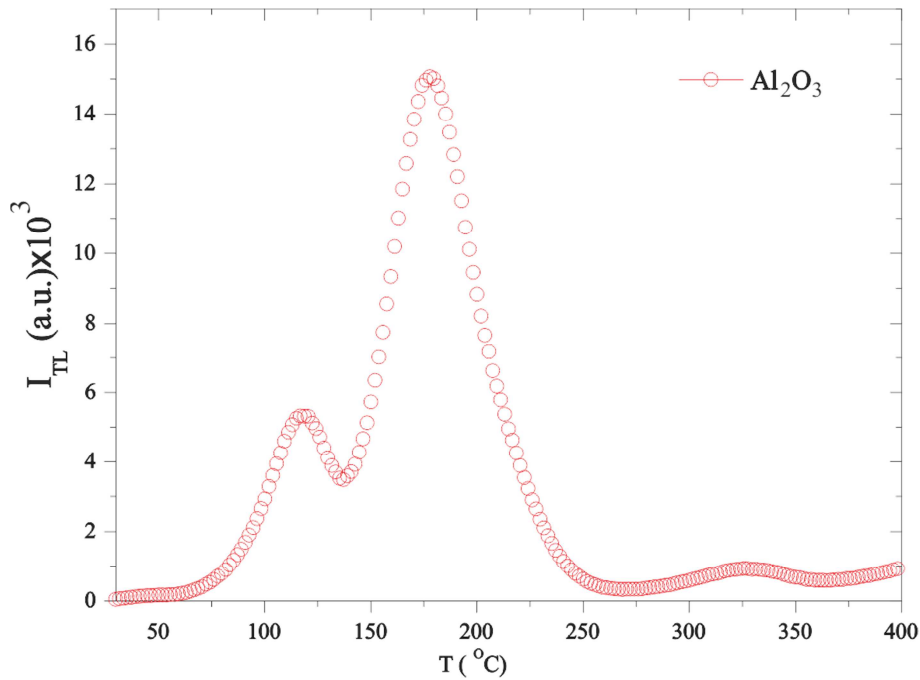


Figure 2. Thermoluminescence glow curve of the α - Al_2O_3 .

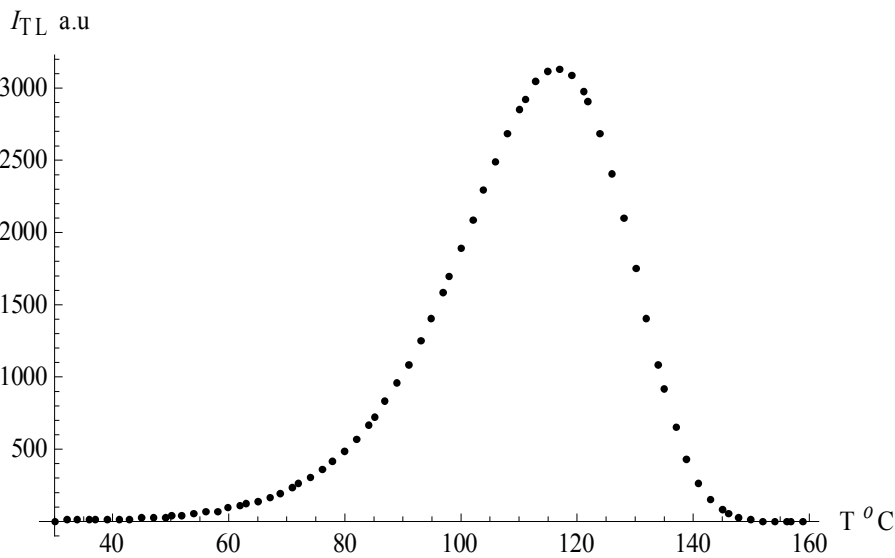


Figure 3. Experimental first order glow curve of α - Al_2O_3 powder: The peak is isolated from others and located at $117 \pm 2^\circ C$. Calculated numerical first order glow curves for $E_c=0.89eV$, $S_c=2.17 \times 10^{10} s^{-1}$, $A_{re}=1$, $n_{co}=0$, $A_{te}=0$, $N=1.17 \times 10^5 cm^3 s^{-1}$, $n_o=1.18 \times 10^5 cm^3 s^{-1}$.

2.3. Numerical Analysis

In this study, all numerical solutions are calculated iteratively. Each solution is started from a given initial particular value of n_o , n_{co} at T_{min} , and then takes a sequence of steps, trying eventually to cover the whole range T_{min} to T_{max} . Numerical simulations are performed by using experimental glow curve and the following experimental parameters: $E_c=0.89eV$, $S_c=2.17 \times 10^{10} s^{-1}$, $N=n_o=1.17 \times 10^5 cm^3 s^{-1}$ and other parameters are chosen realistically. As a result, the initial value for A_{re} is set 1 and A_{te} is set 0 for first order kinetic. Numerical methods used in this work are;

- Explicit Euler [10, 11],
- Generalized Euler [11, 12],

- Classical Runge-Kutta [12, 13],
- Implicit Runge-Kutta [13, 14],
- Explicit Runge-Kutta with Fehlberg coefficients [15]
- and Explicit Runge-Kutta with Bogacki-Shampine coefficients [16, 17] methods.

Simulations of the models are performed in Mathematica 8.1 [18–20].

3. Results

Numerical solutions of the OTOR model are performed by using Explicit Euler, Generalized Euler, Classical Runge-Kutta (3-9 order), Implicit Runge-Kutta (3-9 order), Explicit Runge-Kutta (3-9 order), Explicit Runge-Kutta with

Felberg Coefficients (3-9 order) and Explicit Runge–Kutta with Bogacki-Shampine Coefficients (3-9 order) methods for different step sizes and differential orders. In order to make comparison easier, glow curves of the experiment and simulations are drawn together and figure of merit (FOM) [1, 8] is also calculated. In order to see the difference between the results obtained, the values of FOM are given in many digits. Size of steps are selected as 0.1×10^{-5} - 0.1×10^0 but some of the methods cannot solve the equations for the given set of experimental parameters and glow curve. Therefore glow curve is normalized and size of steps are rearranged for these methods. For instance, size of steps are selected as 2.5×10^{-5} - 0.1×10^{-5} for Explicit Euler, Explicit Runge-Kutta

and Classical Runge-Kutta methods. Additionally, Explicit Euler and Explicit Runge-Kutta methods are also applied to normalized glow curve for size of steps of 0.1×10^{-5} - 0.1×10^0 .

Differential equations of the OTOR model is solved numerically by using Explicit Euler, Generalized Euler, Classical Runge-Kutta, Implicit Runge-Kutta, Explicit Runge–Kutta, Felberg and Bogacki-Shampine methods and results of a number of runs are shown in Figure 4-10, respectively. In each case, numerically calculated glow curve has been compared with experimental glow curve and FOM is calculated. For each of the points illustrated in the figures all of the trapping parameters are held constant as in Table 1 and the size of step is varied, as indicated in the figure captions.

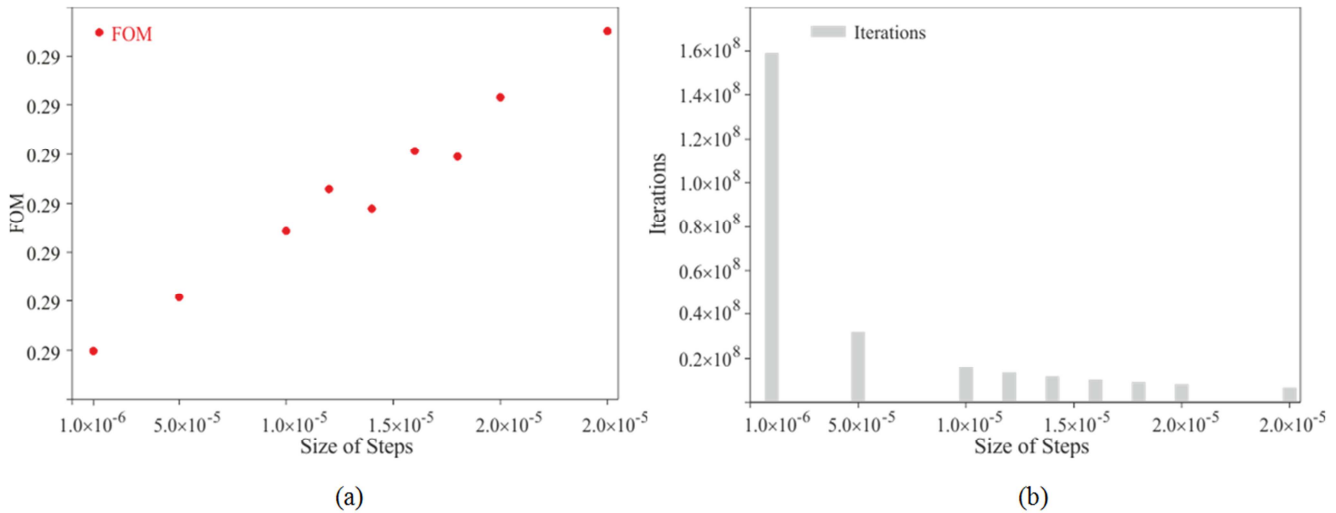


Figure 4. Simulation results of the Explicit Euler method: (a) FOM values are shown as red dots and (b) number of iterations are shown as gray bars. Size of step is varied from 2.5×10^{-5} to 0.1×10^{-5} .

The main point regarding the Figure 4a, b is that the number of iterations and calculating time is related to size of steps. Moreover, FOM value is improved by the decreasing of the size of steps.

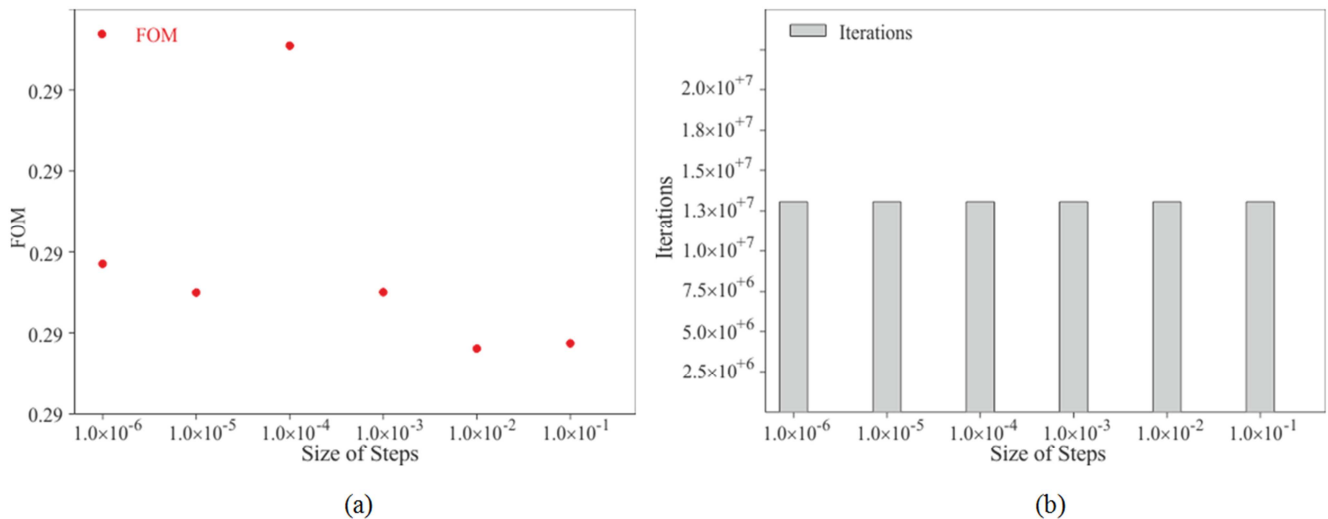


Figure 5. Simulation results of the Generalized Euler method: (a) FOM values are shown as red dots and (b) number of iterations are shown as gray bars. Size of step is varied from 1.0×10^1 to 0.1×10^{-5} .

In Figure 5a, b we find that even when size of steps are varied, the number of iterations and calculating times remain nearly constant. The best FOM value is calculated when size of steps is equals to 1.0×10^{-2} .

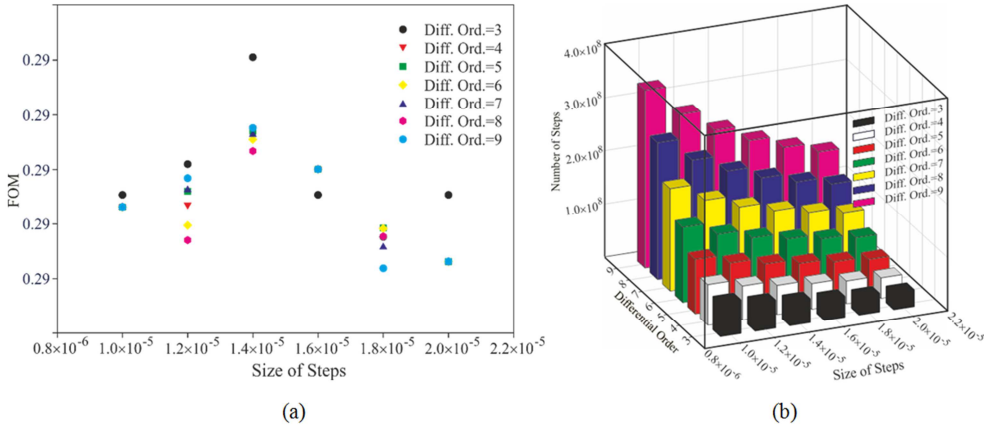


Figure 6. Simulation results of the Classical Runge-Kutta method: (a) FOM values are shown as red dots and (b) number of iterations are shown as gray bars. Size of step is varied from 2.0×10^{-5} to 1.0×10^{-6} .

It is easy to see from the Figure 6a, b that the number of iteration and calculating time are varied with size of step and differential order. Here, the best FOM value is calculated when size of step and differential order equals to 1.8×10^{-5} and 9, respectively.

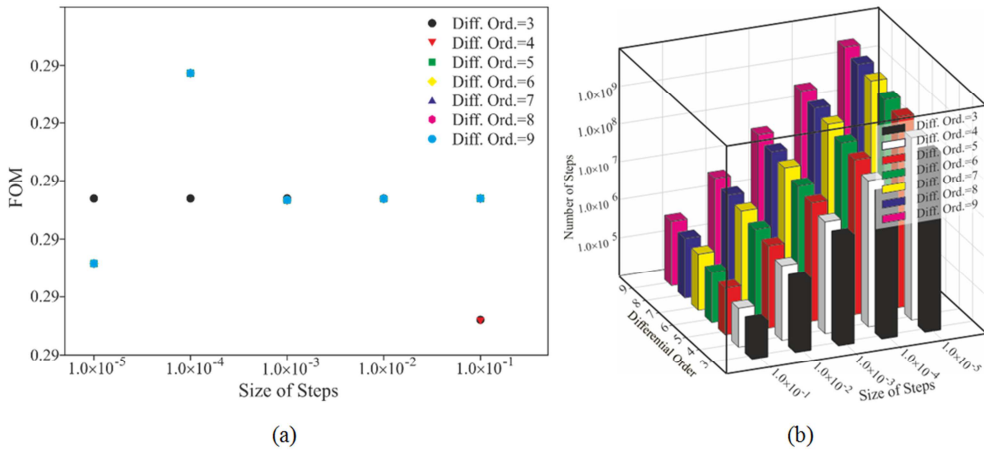


Figure 7. Simulation results of the Implicit Runge-Kutta method: (a) FOM values are shown as red dots and (b) number of iterations are shown as gray bars. Size of step is varied from 1.0×10^{-1} to 1.0×10^{-6} .

From Figure 7a and b, obviously, the number of iteration and calculating time are increased with size of step and differential order. For the method the best FOM value is calculated when size of step and differential order equals to 3×10^{-1} and 3, respectively.

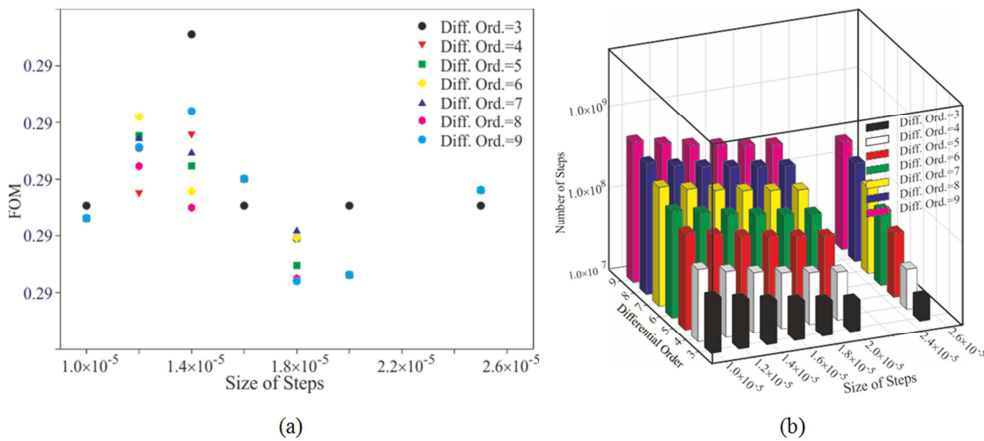


Figure 8. Simulation results of the Explicit Runge-Kutta method: (a) FOM values are shown as red dots and (b) number of iterations are shown as gray bars. Size of step is varied from 2.5×10^{-5} to 1.0×10^{-5} .

From Figure 8a and b, it is concluded that the number of iteration and calculating time are increased with size of step and differential order. Besides, the best FOM value is calculated when size of step and differential order equals to 1.8×10^{-5} and 9, respectively.

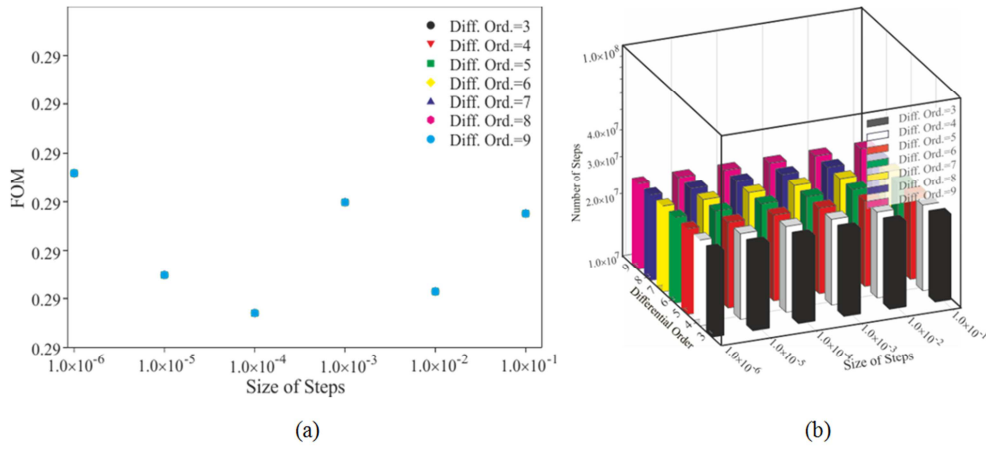


Figure 9. Simulation results of the Fehlberg Method: (a) FOM values are shown as red dots and (b) number of iterations are shown as gray bars. Size of step is varied from 1.0×10^{-1} to 1.0×10^{-6} .

Results of a number of runs in Figure 10a, b show that although the number of iteration and calculating time is independent of step size, it is increased by differential order. Additionally, the best FOM value is calculated when size of step and differential order equals to 1.8×10^{-5} and 9, respectively.

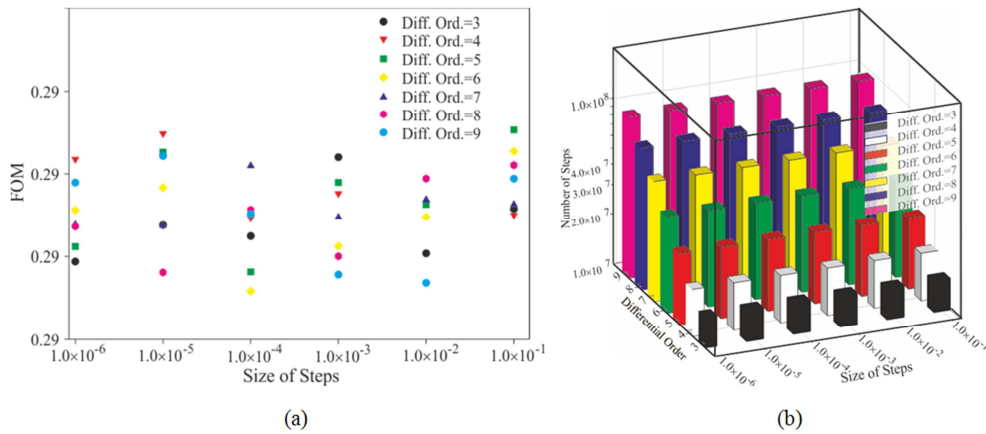


Figure 10. Simulation results of the Bogacki-Shampine Method: (a) FOM values are shown as red dots and (b) number of iterations are shown as gray bars. Size of step is varied from 1.0×10^{-1} to 1.0×10^{-6} .

Like in the previously discussed results of the Fehlberg Method, from Figure 10a, b one can be seen that although the number of iteration and calculating time is independent of step size, it is increased by differential order. Additionally, the best FOM value is calculated when size of step and differential order equals to 1×10^{-3} and 6, respectively.

4. Discussions

The results obtained by applying the Explicit Euler method to the OTOR model show that if size of step is smaller than 2.5×10^{-5} , differential equations set of the model can be solved numerically for the given set of initial parameters. Results show that FOM value is decreased by the decreasing of the size of steps. In the simulations, the smallest size of step is taken as 0.1×10^{-5} and the best FOM value is calculated for

$\sim 1.59 \times 10^8$ iterations. Even though smaller step size give more accurate FOM value, number of iteration and calculation time are increases. For instance when size of step decreases from 0.5×10^{-5} to 0.1×10^{-5} , number of iteration increases nearly five times. Although using the small step size increases the calculation time, it causes an improvement of the FOM value.

On the other hand, numerical solutions of the OTOR model by performing Generalized Euler method show that number of iteration is not depend on size of step. Note that $\sim 1.30 \times 10^7$ iterations are performed if size of step is equal to 1.0×10^{-1} whereas $\sim 1.30 \times 10^7$ iterations are performed if size of step is equal to 0.1×10^{-5} . Although there are no any limitation for the size of step for given initial parameters, the best value of FOM is calculated for step size of 1.0×10^{-2} and it is in excellent agreement with the experimental result.

Results of the Classical Runge-Kutta method for different size of step and differential order show that number of iteration is heavily depend on size of step and differential order of the method together. For example, when size of step decreases from 2×10^{-5} to 1×10^{-5} , number of iteration increases nearly doubles for all order of Classical Runge-Kutta methods. In addition, although the same size of step is used, number of iteration is also increased by using higher-order Classical Runge-Kutta method. For example, when differential order is equal to 3, $\sim 6.36 \times 10^7$ iterations are performed for step size of 10^{-5} . When differential orders is equal to 9, $\sim 2.57 \times 10^8$ iterations are performed for the same step size of 10^{-5} . Even though the number of iteration increases with the decreasing of the step size, no improvement in FOM value is observed. Moreover, the best FOM result is calculated at low iteration number. Besides, the best FOM value is calculated when step size is equal to 1.8×10^{-5} for third order Classical Runge-Kutta method. Nevertheless the best FOM values are calculated when step size is equal to 2.0×10^{-5} for all other order Classical Runge-Kutta methods.

The conclusions obtained by employing the Implicit Runge-Kutta method to the OTOR model for different size of steps and differential orders show that there are no restrictions for the size of step for given initial parameters. Therefore the size of step can be selected in wide range from 0.1 to 1.0×10^{-6} without performing any data manipulation such as normalization. On the other hand, size of step and differential order of the method are strongly have an effect on number of iteration. For instance, when size of step decreases from 10^{-1} to 1×10^{-5} , number of iteration increases from $\sim 9.14 \times 10^3$ to $\sim 5.58 \times 10^6$. Besides, number of iteration is also increased by using higher-order methods for the same size of step. Although the best FOM value is calculated by using step size of 1×10^{-1} for third and fourth order Implicit Runge-Kutta, it is calculated by using step size of 1×10^{-3} for all other order Implicit Runge-Kutta methods.

Results of the numerical simulations of the Explicit Runge-Kutta method show that if size of step is smaller than 2.5×10^{-5} , differential equations set of the model can be solved numerically for the given set of initial parameters. Besides, number of iteration is closely related to size of step and differential order of the Explicit Runge-Kutta method together. When size of step decreases, number of iterations increases. For instance, if size of step decreases from 2×10^{-5} to 1×10^{-5} , number of iteration increases from $\sim 1.44 \times 10^8$ to $\sim 2.88 \times 10^8$, nearly doubles for seventh-order Explicit Runge-Kutta method. Moreover, although the same size of step is used, number of iteration is also increased by using the higher-order method. For example, when differential order is equal to 3, $\sim 4.77 \times 10^7$ iterations are performed for step size of 10^{-5} . When ninth-order Explicit Runge-Kutta method is used, $\sim 5.25 \times 10^8$ iterations are performed for the same step size of 10^{-5} . It is important to point out that improvement in FOM value is not observed when size of step is less than 1.8×10^{-5} . Indeed, improvement of the FOM value is not a linear function of the number of iteration or size of step. For

instance, for third, eight and ninth order of Explicit Runge-Kutta methods, the best FOM value is calculated when step size is equal to 1.8×10^{-5} . However, the best FOM value is calculated when step size is equal to 2.0×10^{-5} for all other order Explicit Runge-Kutta methods.

Simulation results on Fehlberg Method show that number of iteration is independent of the size of step and differential order of the method. For instance, although size of step decreases from 1×10^{-1} to 1×10^{-6} , number of iteration is nearly constant at $\sim 2.57 \times 10^7$. Moreover, even if higher order methods are used, number of iteration is also nearly constant. For example, when differential order is equal to 3, $\sim 2.57 \times 10^7$ iterations are performed for step size of 10^{-6} . When differential orders are equal to 9, $\sim 2.57 \times 10^7$ iterations are performed for the same step size. Moreover, the best FOM values are calculated for the same step size even if order of the method is different. For instance, the best FOM values are calculated when step size is equal to 1.0×10^{-4} for all order of Fehlberg methods.

Numerical simulation results of the Bogacki-Shampine Method show that although the number of iteration is firmly related to differential order of the method, it is independent of the size of step. Besides, it is observed that a low order method require less iteration nevertheless higher order method needs more iteration. For instance, if order of the method increases from 3 to 9, number of iterations increases from $\sim 1.54 \times 10^7$ to $\sim 9.44 \times 10^7$, more than sixth times for size of step of 10^{-6} .

The results obtained by applying the Explicit Euler, Classical and Explicit Runge-Kutta methods to the OTOR model show that if size of step is smaller than 2.5×10^{-5} , differential equations set of the model can be solved numerically for the given set of initial parameters. On the other hand, an overflow error is observed when the size of steps have a value greater than 2.5×10^{-5} . Simulations show that relatively big n_0 values are caused overflow error for the three methods. On the other hand, simulations also show that if sufficiently small n_0 values are used, bigger size of steps can also be employed. Here, it is interesting to note that, although peak height and area under the glow curve are affected by n_0 , the other characteristics of the glow curves are independent of n_0 values. Therefore, Explicit Euler and Explicit Runge-Kutta methods can be applied for relatively big n_0 values, when glow curves and initial n_0 values are normalized. For instance; in this work, experimental glow curves and initial n_0 values are normalized by using $2 \times I_{\max}$ and Explicit Euler and Explicit Runge-Kutta methods can be applied to the OTOR model for bigger step sizes such as 10^{-1} - 10^{-4} .

5. Conclusions

In this work the best FOM value is calculated by using ninth-order Classical Runge-Kutta method for size of step is 1.8×10^{-5} after 1.86×10^8 iterations. On the other hand, if Explicit Euler method is used for the same step size, FOM value is calculated $7.29 \times 10^{-3}\%$ times greater than the best one after the 8.83×10^6 iterations. Obviously, although the

difference between the FOM values is very small, the calculating time of the ninth-order Classical Runge-Kutta method is extremely longer than Explicit Euler method. The shortness of calculation time seems to be a good criterion with FOM value, and it will also help us in determining the best numerical method for OTOR model.

Acknowledgements

This work has been funded by Karamanoğlu Mehmetbey University Commission of Scientific Research Projects (Project Number: 20-M-16).

References

- [1] S. W. S. McKeever, *Thermoluminescence of Solids*, Cambridge University Press, Cambridge, 1985. doi: 10.1017/CBO9780511564994.
- [2] R. Chen, S. W. S. McKeever, *Theory of Thermoluminescence and Related Phenomena*, 1997. doi: 10.1142/2781.
- [3] R. Chen, V. Pagonis, *Thermally and Optically Stimulated Luminescence: A Simulation Approach*, 2011. doi: 10.1002/9781119993766.
- [4] P. J. Kemmey, P. D. Townsend, P. W. Levy, Numerical analysis of charge-redistribution processes involving trapping centers, *Phys. Rev.* 155 (1967) 917–920. doi: 10.1103/PhysRev.155.917.
- [5] P. Kelly, M. J. Laubitz, P. Bräunlich, Exact solutions of the kinetic equations governing thermally stimulated luminescence and conductivity, *Phys. Rev. B.* 4 (1971) 1960–1968. doi: 10.1103/PhysRevB.4.1960.
- [6] D. Shenker, R. Chen, Numerical solution of the glow curve differential equations, *J. Comput. Phys.* 10 (1972) 272–283. doi: 10.1016/0021-9991(72)90066-6.
- [7] R. Chen, W. F. Hornyak, V. K. Mathur, Competition between excitation and bleaching of thermoluminescence, *J. Phys. D. Appl. Phys.* 23 (1990) 724–728. doi: 10.1088/0022-3727/23/6/015.
- [8] H. G. Balian, N. W. Eddy, Figure-of-merit (FOM), an improved criterion over the normalized chi-squared test for assessing goodness-of-fit of gamma-ray spectral peaks, *Nucl. Instruments Methods.* 145 (1977) 389–395. doi: 10.1016/0029-554X(77)90437-2.
- [9] S. W. S. McKeever, *Thermoluminescence of Solids*, Cambridge University Press, Cambridge, 1985. doi: 10.1017/CBO9780511564994.
- [10] J. D. Hoffman, Numerical Differentiation and Difference Formulas, in: *Numer. Methods Eng. Sci.*, Second Edi, Marcel Dekker, Inc, NEW YORK. BASEL, 2001: pp. 257-270.
- [11] J. Bulirsch, R. Stoer, Ordinary Differential Equations, in: J. E. Marsden, M. Golubitsky, L. Sirovich, W. Jager (Eds.), *Introd. to Numer. Anal.*, Second Edi, Springer-Verlag New York, Inc., New York, 1992: pp. 434-471.
- [12] W. H. Press, S. A. Teukolsky, W. T. Vetterling, B. P. Flannery, Integration of Ordinary Differential Equations, in: W. H. Press, S. A. Teukolsky, W. T. Vetterling, B. P. Flannery (Eds.), *Numer. Recipes Fortran 77 Art Sci. Comput.*, Second Edi, Press Syndicate of the University of Cambridge, Cambridge, 1997: pp. 704-716.
- [13] S. D. Conte, C. de Boor, The Solution of Differential Equations, in: S. D. Conte, C. de Boor (Eds.), *Elem. Numer. Anal. An Algorithmic Approach*, Third Edit, McGraw-Hill, inc., New York, 1980: pp. 354-370.
- [14] L. F. Shampine, Some Practical Runge-Kutta Formulas, *Math. Comput.* 46 (1986) 135. doi: 10.2307/2008219.
- [15] E. Fehlberg, Classical fifth-, sixth-, seventh-, and eighth-order Runge-Kutta formulas with stepsize control, *NASA Tech. Rep.* (1968) R-287. doi: 10.1007/BF02234758.
- [16] P. Bogacki, L. Shampine, A 3 (2) Pair of Runge-Kutta Formulas, *Appl Math Lett.* 2 (1989) 321–325. doi: 10.1016/0893-9659(89)90079-7.
- [17] P. Bogacki, L. F. Shampine, An efficient Runge-Kutta (4, 5) pair, *Comput. Math. with Appl.* 32 (1996) 15–28. doi: 10.1016/0898-1221(96)00141-1.
- [18] J. Nearing, *Mathematical Tools for Physics, Analysis.* 30 (2003) 1316–22. doi: 10.1002/3527607773.
- [19] M. Sofroniou, R. Knapp, Advanced Numerical Differential Equation Solving in Mathematica, ... Inc. URL [Http/reference. Wolfram. Com/mathematica/](http://reference.wolfram.com/mathematica/) (2008). <http://scholar.google.com/scholar?hl=en&btnG=Search&q=intitle:ADVANCED+NUMERICAL+DIFFERENTIAL+EQUATION+SOLVING+IN+MATHEMATICA#1>.
- [20] M. Trott, *The Mathematica GuideBook for Numerics*, Springer New York, New York, NY, 2006. doi: 10.1007/0-387-28814-7.